Keio University

Kinetic Modeling of Classical and Neo-Classical Transport for High-Z impurities in Fusion SOL/Divertor Plasmas using Binary Collision Method

第20回NEXT研究会
2015/1/13-14
京都テルサ、京都

Yuki HOMMA,
Yu SAWADA,
Shohei YAMOTO,
Akiyoshi HATAYAMA.

Keio Univertisy, Tokyo, Japan.

Table of Contents

1. Introduction

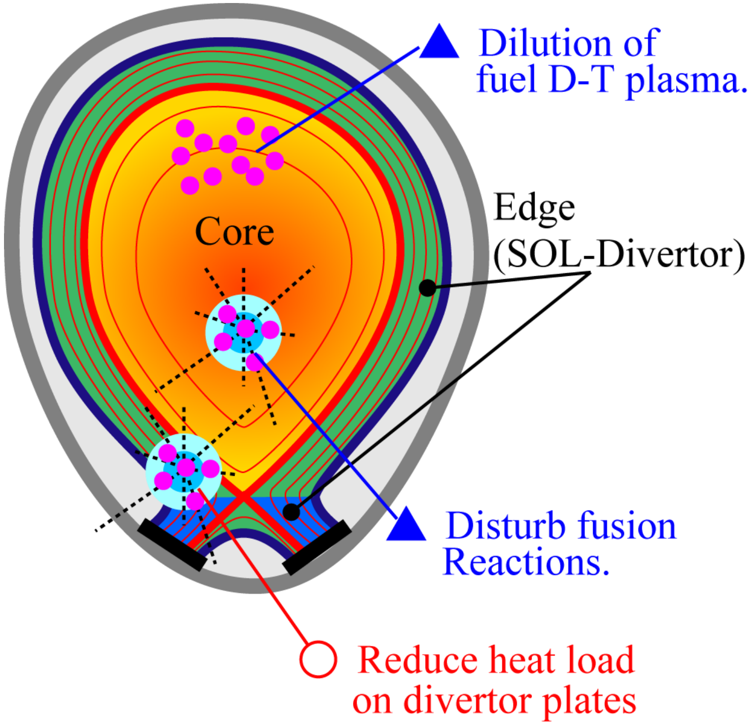

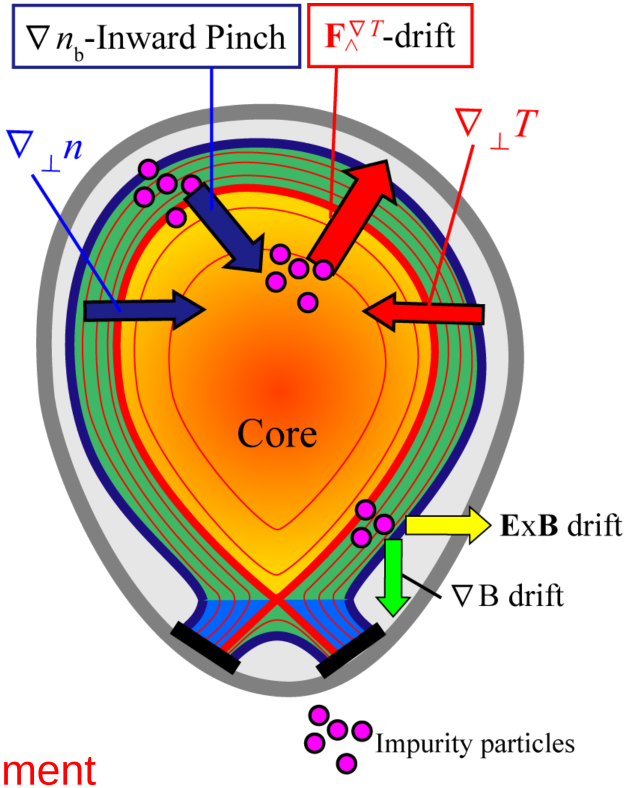

=> Useful for divertor development

- Correct understanding of impurity (imp.) transport in SOL/Divertor region is important for developing fusion devices.

- Focus on Neo-classical transport of high-Z impurities.

1. IWP vs. TSE

-- Classical (CL) & Neoclassical (NC) cross-field imp. transport:
Inward Pinch (IWP) vs. Temperature Screening Effect (TSE) [1]

Transport	Trigger	Direction	Effect
CL/NC IWP	B.g. ∇n_b	$// \nabla n_b$ (to high n_b)	Accumulation
CL/NC TSE	B.g. ∇T_b	$//(-\nabla T_b)$ (to low T_b)	Exclusion
CL/NC Self Diffusion	Imp. ∇n_Z	$//(-\nabla n_Z)$	Flatten n_Z (weaker for high Z imp.)

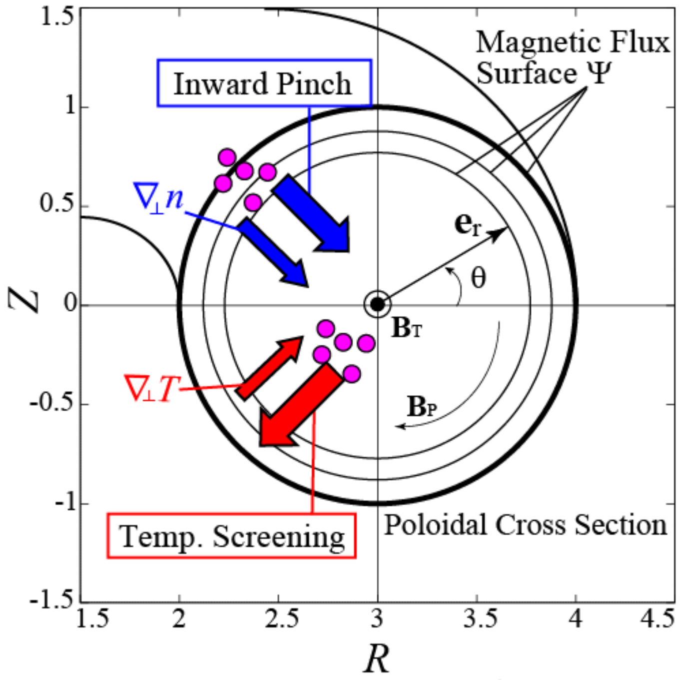

Fig 1. Simple Torus Magnetic Field

$$\mathbf{B} = \mathbf{B}_t + \mathbf{B}_p \begin{cases} \mathbf{B}_t = -\dfrac{B_0 R_0}{R}\mathbf{e}_\varphi \\ \mathbf{B}_p = -\dfrac{\mu_0 R_0 I_p}{2\pi R r}\mathbf{e}_\theta \end{cases}$$

Magnetic Drift (Downward) $\mathbf{V}_a^{\nabla B \mathrm{drift}} \cong -\dfrac{2T_a}{e_a R B}\mathbf{e}_Z$

-- NC transport theory is established under *closed* **B** configuration.

1. Purpose of Study

① Develop a CL&NC transport simulation model for test impurity particles.

IWP&TSE have not been included in most impurity transport simulations...

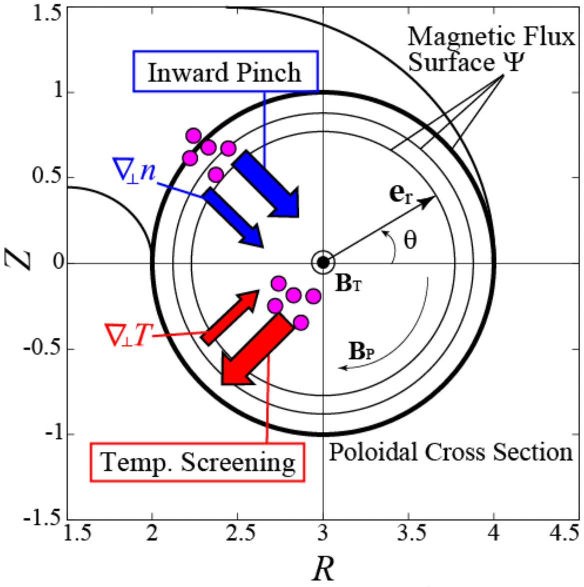

Fig 1. Simple Torus Magnetic Field

Other transport processes such as ExB drift or anomalous diffusion are not considered in this study.

2. Neoclassical Impurity Transport Theory

Theory

$$\left\langle \mathbf{V}_Z \cdot \mathbf{e}_r \right\rangle^{NC} = \frac{\left\langle \mathbf{\Gamma}_Z \cdot \mathbf{e}_r \right\rangle^{NC}}{n_Z} \cong 2q_{\text{safety}}^2 Z D_b^{\text{CL}} \left[\underset{\text{NC IWP}}{\boxed{0.9\frac{\nabla_\perp n_b}{n_b}}} \underset{\text{NC TSE}}{\boxed{-0.59\frac{\nabla_\perp T_b}{T_b}}} \right]$$

derived based on Ref. [1].

- B.g. plasma in Pfirsch-Schluter regime
- Collisional force on impurity from plasma ions : $\mathbf{R}_{Z,\parallel} = n_Z \mathbf{F}_{Z,\parallel} = 0.9\frac{m_b n_b}{\tau_{bZ}}\left(\mathbf{V}_b - \mathbf{V}_Z\right) + 1.89 n_b \nabla_\parallel T_b$
- Effective charge state : $Z_{eff} := \left(n_b e_b^2 + n_Z e_Z^2\right) / n_e e_e^2 = 2$

NC Mechanisms of NC IWP & NC TSE => next …

2. Mechanism of NC IWP

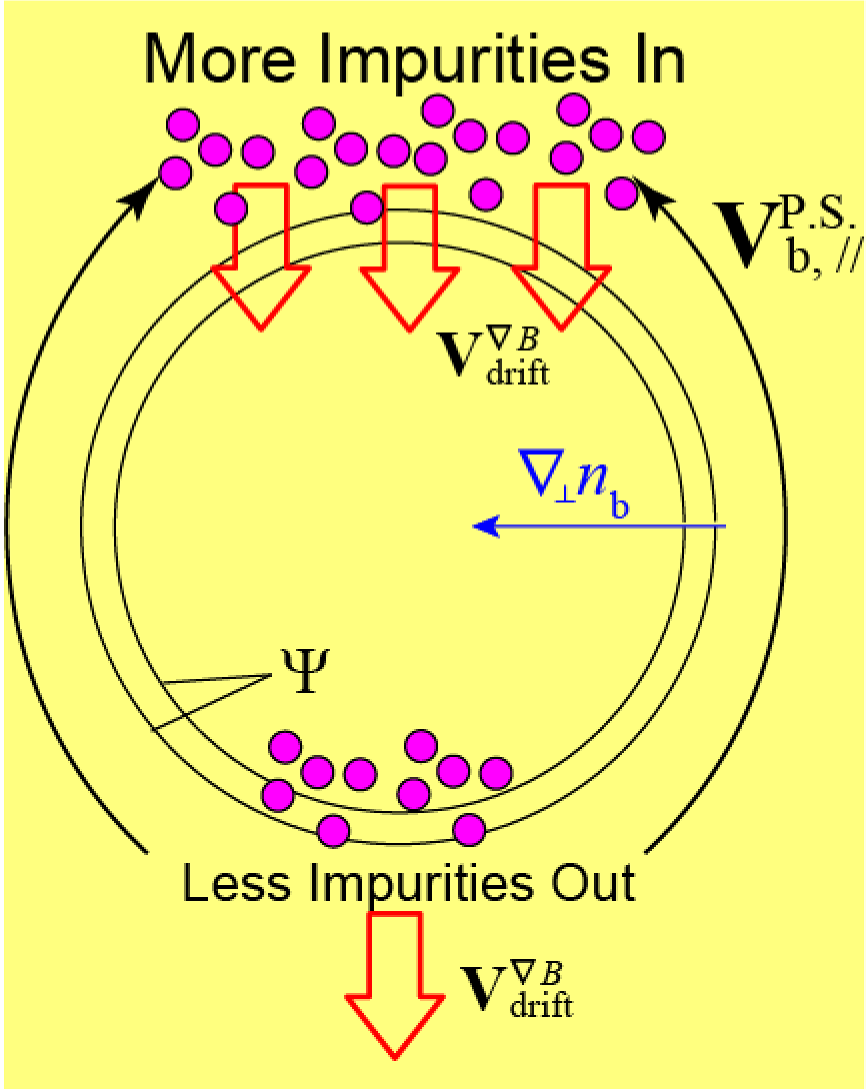

Fig 2. Neoclassical Inward Pinch (NC IWP)

1. Under $\nabla_{\perp} n_b$ & diamag. drift flow $V_{b,\wedge}$, Pfirsch-Schluter plasma flow arises,

$$\mathbf{V}_{b,\parallel}^{\text{P.S.}} = \frac{2q_{safety}}{n_b e_b B} \cos\theta \frac{dp_b}{dr} \cdot \left(\frac{\mathbf{B}}{B} \right), \qquad p_b := n_b T_b ,$$

to fulfill $\nabla \cdot (n_b \mathbf{V}_b) = \nabla \cdot \left(n_b \mathbf{V}_{b,\wedge} + n_b \mathbf{V}_{b,\parallel}^{P.S.} \right) = 0$.

2. PS flow drives imps. toward the top.

3. More imps. on Top of cross-section, less imps. on Bottom.
Near Top, mag. drift $V^{\nabla B}$ Inward,
Near Bottom, $V^{\nabla B}$ Outward.

4. Unbalanced contribution of each $V^{\nabla B}$.
=> Net radial INWARD flow of imps.
NC IWP.

2. Mechanism of NC TSE

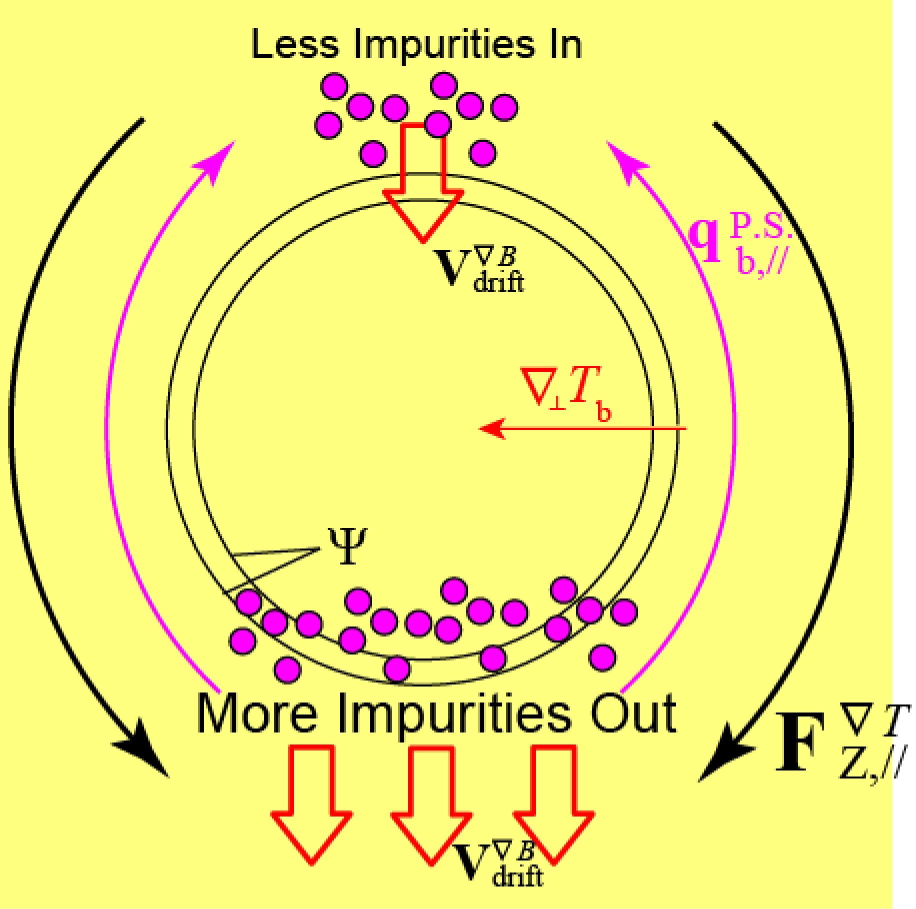

Fig 3. Neoclassical Temperature Screening Effect (NC TSE)

1. Under $\nabla_\perp T_b$ & diamag. heat flux $q_{b,\wedge}$, Pfirsch-Schluter heat flux arises,
$$\mathbf{q}_{b,\|}^{\text{P.S.}} = \frac{5n_bT_b}{e_bB} q_{safety} \cos\theta \cdot \frac{dT_b}{dr} \cdot \left(\frac{\mathbf{B}}{B}\right),$$
with the assumption that
$$\nabla \cdot \left(\mathbf{q}_b\right) = \nabla \cdot \left(\mathbf{q}_{b,\wedge}^{\text{Diamag}} + \mathbf{q}_{b,\|}^{\text{P.S.}}\right) = 0.$$

2. PS heat flux generates parallel thermal force [4] $\mathbf{F}_{\|,Z}^{\nabla T} \propto -\mathbf{q}_{b,\|}$.

3. More imps. on Bottom, less imps. on Top.

4. Unbalanced $V^{\nabla B}$ averaged
=> Net radial OUTWARD flow of imps.
NC TSE.

3. Simulation Model for NC Transport

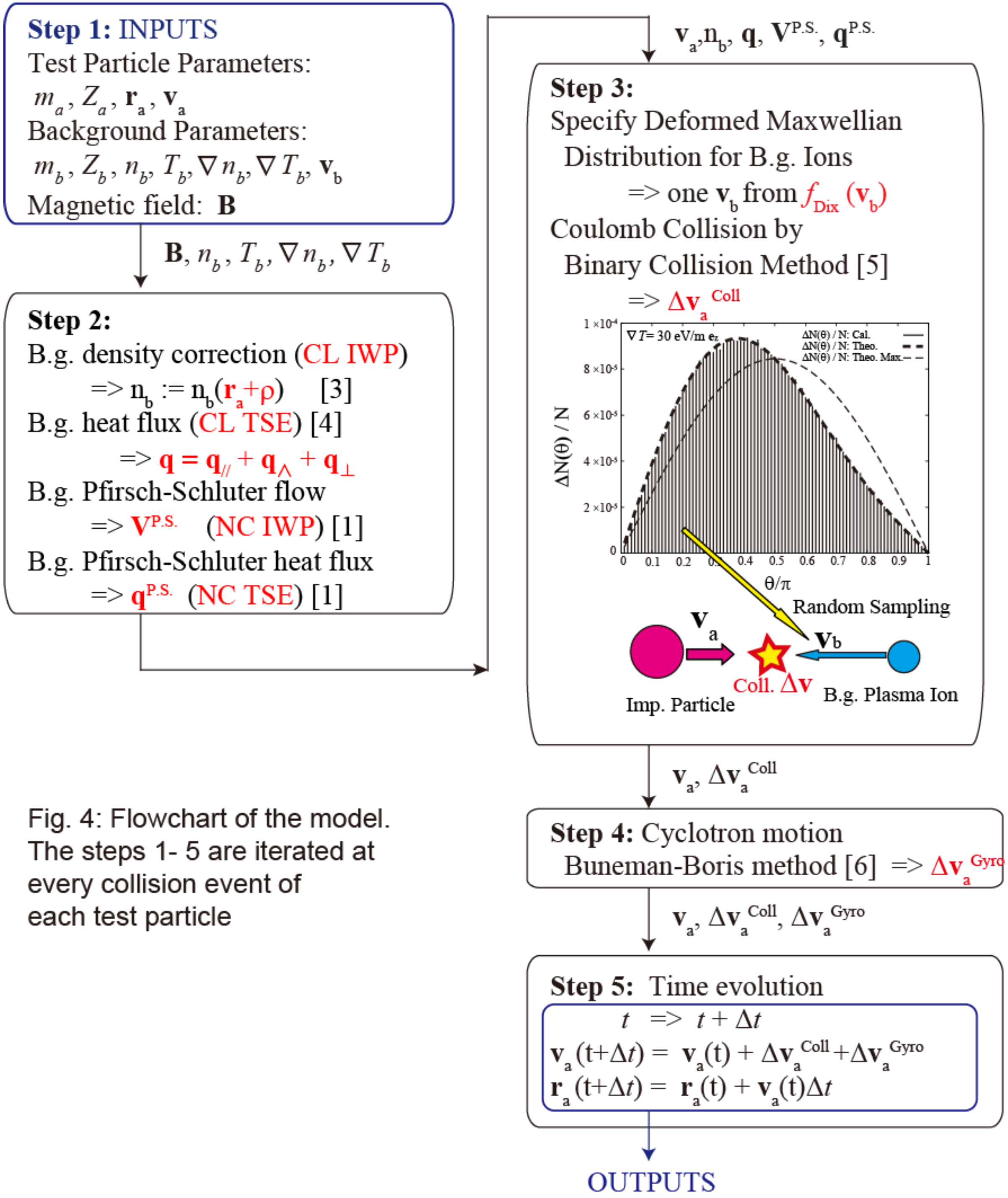

Step 1: INPUTS
Test Particle Parameters:
m_a, Z_a, $\mathbf{r}_a$, $\mathbf{v}_a$
Background Parameters:
m_b, Z_b, n_b, T_b, ∇n_b, ∇T_b, $\mathbf{v}_b$
Magnetic field: **B**

$\mathbf{B}$, n_b, T_b, ∇n_b, ∇T_b

Step 2:
B.g. density correction (CL IWP)
=> $n_b := n_b(\mathbf{r}_a+\rho)$ [3]
B.g. heat flux (CL TSE) [4]
=> $\mathbf{q} = \mathbf{q}_{//} + \mathbf{q}_{\wedge} + \mathbf{q}_{\perp}$
B.g. Pfirsch-Schluter flow
=> $\mathbf{V}^{P.S.}$ (NC IWP) [1]
B.g. Pfirsch-Schluter heat flux
=> $\mathbf{q}^{P.S.}$ (NC TSE) [1]

$\mathbf{v}_a$, n_b, $\mathbf{q}$, $\mathbf{V}^{P.S.}$, $\mathbf{q}^{P.S.}$

Step 3:
Specify Deformed Maxwellian
Distribution for B.g. Ions
=> one $\mathbf{v}_b$ from $f_{Dix}(\mathbf{v}_b)$
Coulomb Collision by
Binary Collision Method [5]
=> $\Delta\mathbf{v}_a^{Coll}$

$\mathbf{v}_a$, $\Delta\mathbf{v}_a^{Coll}$

Step 4: Cyclotron motion
Buneman-Boris method [6] => $\Delta\mathbf{v}_a^{Gyro}$

$\mathbf{v}_a$, $\Delta\mathbf{v}_a^{Coll}$, $\Delta\mathbf{v}_a^{Gyro}$

Step 5: Time evolution

$$t \Rightarrow t+\Delta t$$
$$\mathbf{v}_a(t+\Delta t) = \mathbf{v}_a(t) + \Delta\mathbf{v}_a^{Coll} + \Delta\mathbf{v}_a^{Gyro}$$
$$\mathbf{r}_a(t+\Delta t) = \mathbf{r}_a(t) + \mathbf{v}_a(t)\Delta t$$

OUTPUTS

Fig. 4: Flowchart of the model.
The steps 1- 5 are iterated at
every collision event of
each test particle

3. Distorted Maxwellian for Background plasma ion velocity

Step 3:

Specify Deformed Maxwellian Distribution for B.g. Ions

=> one $\mathbf{v}_b$ from f_{Dix} $(\mathbf{v}_b)$

Coulomb Collision by Binary Collision Method [5]

=> $\Delta \mathbf{v}_a^{\mathrm{Coll}}$

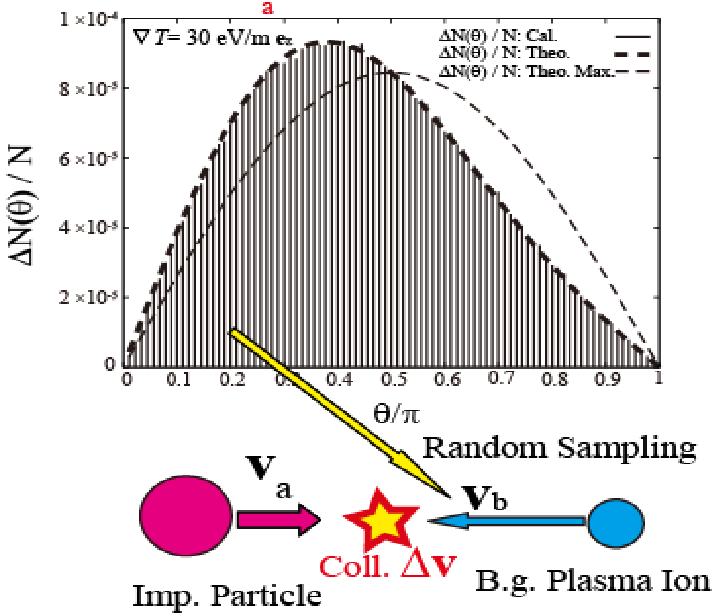

Random sampling of v_b from

Distorted (Deformed) Maxwellian for background plasma ion velocity

$$f_b(\boldsymbol{v}) = \underbrace{n_b\left(\frac{m_b}{2\pi T_b}\right)^{3/2}\exp\left(-\frac{m_b v^2}{2T_b}\right)\times}_{\text{Maxwellian}}\underbrace{\left[1-\frac{m_b}{n_b}\frac{1}{T_b^2}\left(1-\frac{v^2}{5v_{th,b}^2}\right)(\boldsymbol{q}\cdot\boldsymbol{v})\right]}_{\text{Distortion due to } \nabla T}$$

4. Test Simulation of NC Transport, Closed B-field

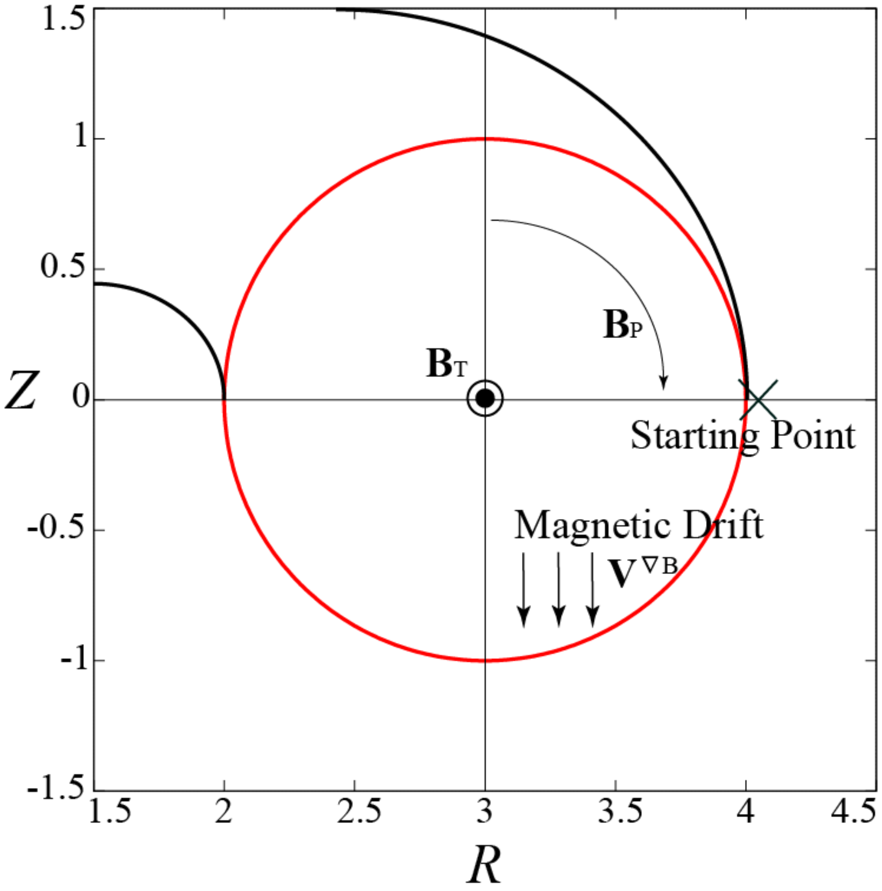

Fig. 5:
Torus magnetic B-field

Impurities start moving from the outer mid-plane
(R, θ, φ) = (1.05, 0, 0).

Time evolution of av. minor radius

vs. Theory dr/dt

$$\frac{\Delta\langle r\rangle_{\mathrm{Cal}}}{\Delta t} := \frac{\sum_{i=1}^{N} r_i \big/ N}{\Delta t}.$$

4. Test Simulation of NC Transport, Closed B-field

TABLE I: TEST SIMULATION I, PARAMETERS

Test Impurity Particle Species	W^{4+}
Initial Impurity Velocity $\mathbf{v}_a$	Maxwellian of 100 eV
No. of Test Impurity Particles N	2000
B.g. Plasma Ion Species	D^{1+}
B.g. Plasma Ion Density n_b	$5\times10^{19}\mathrm{m}^{-3}$
B.g. Plasma Temperature	100eV
B.g. Density Gradient ∇n	Given at each case
B.g. Temperature Gradient ∇T	Given at each case
B.g. Plasma Flow except for PS Flow	0 m/s
Magnetic Field Strength B	about 3 T
Collisionality	Pfirsch-Schluter regime
Simulation Time Step Δt	9.04×10^{-9} s
Total Calculation Time	0 s < t< 0.07 s

W/O Limiter, Closed **B**-field

(a) IWP > TSE

$\nabla_\perp n_b = -2\times10^{20}\mathrm{m}^{-3}\cdot\mathbf{e}_r(=4n_b),$

$\nabla_\perp T_b = -300\mathrm{eV/m}\cdot\mathbf{e}_r(=3T_b).$

(b) TSE > IWP

$\nabla_\perp n_b = -10^{20}\mathrm{m}^{-3}\cdot\mathbf{e}_r(=2n_b),$

$\nabla_\perp T_b = -600\mathrm{eV/m}\cdot\mathbf{e}_r(=6T_b).$

(c) Cancel (IWP = TSE)

$\nabla_\perp n_b = -10^{20}\mathrm{m}^{-3}\cdot\mathbf{e}_r(=2n_b),$

$\nabla_\perp T_b = -300\mathrm{eV/m}\cdot\mathbf{e}_r(=3T_b).$

W/O Limiter, Closed **B**-field

(a) IWP > TSE

$\nabla_\perp n_b = -2\times10^{20}\mathrm{m}^{-3}\cdot\mathbf{e}_r(=4n_b),$
$\nabla_\perp T_b = -300\mathrm{eV/m}\cdot\mathbf{e}_r(=3T_b).$

(b) TSE > IWP

$\nabla_\perp n_b = -10^{20}\mathrm{m}^{-3}\cdot\mathbf{e}_r(=2n_b),$
$\nabla_\perp T_b = -600\mathrm{eV/m}\cdot\mathbf{e}_r(=6T_b).$

(c) Cancel (IWP = TSE)

$\nabla_\perp n_b = -10^{20}\mathrm{m}^{-3}\cdot\mathbf{e}_r(=2n_b),$
$\nabla_\perp T_b = -300\mathrm{eV/m}\cdot\mathbf{e}_r(=3T_b).$

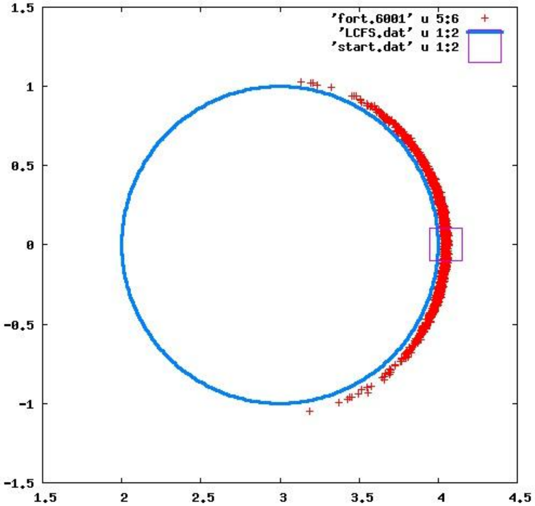

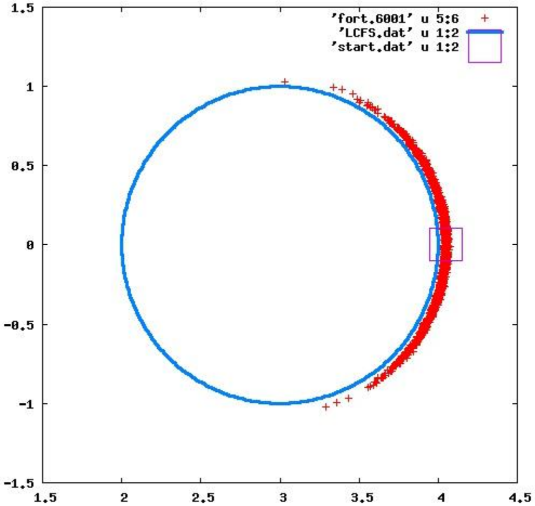

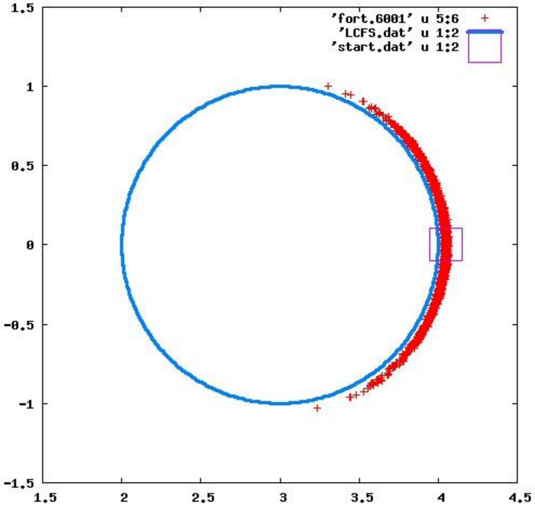

W/O Limiter, Closed **B**-field

(a) IWP > TSE

$\nabla_\perp n_b = -2\times 10^{20}\mathrm{m}^{-3}\cdot\mathbf{e}_r(=4n_b),$

$\nabla_\perp T_b = -300\mathrm{eV/m}\cdot\mathbf{e}_r(=3T_b).$

(b) TSE > IWP

$\nabla_\perp n_b = -10^{20}\mathrm{m}^{-3}\cdot\mathbf{e}_r(=2n_b),$

$\nabla_\perp T_b = -600\mathrm{eV/m}\cdot\mathbf{e}_r(=6T_b).$

(c) Cancel (IWP = TSE)

$\nabla_\perp n_b = -10^{20}\mathrm{m}^{-3}\cdot\mathbf{e}_r(=2n_b),$

$\nabla_\perp T_b = -300\mathrm{eV/m}\cdot\mathbf{e}_r(=3T_b).$

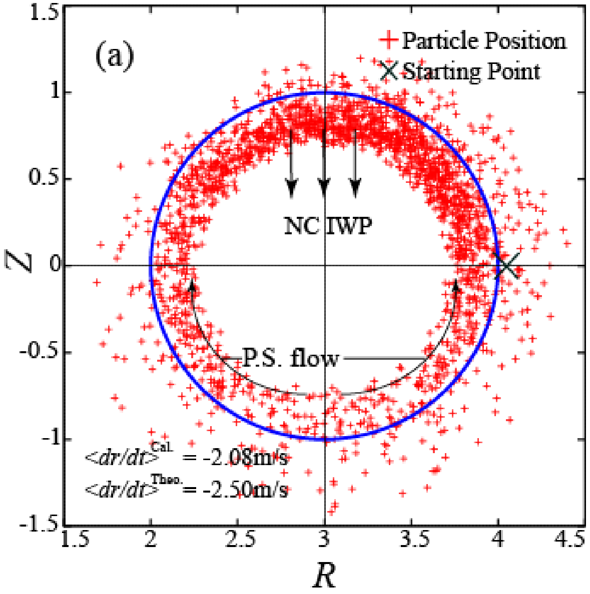

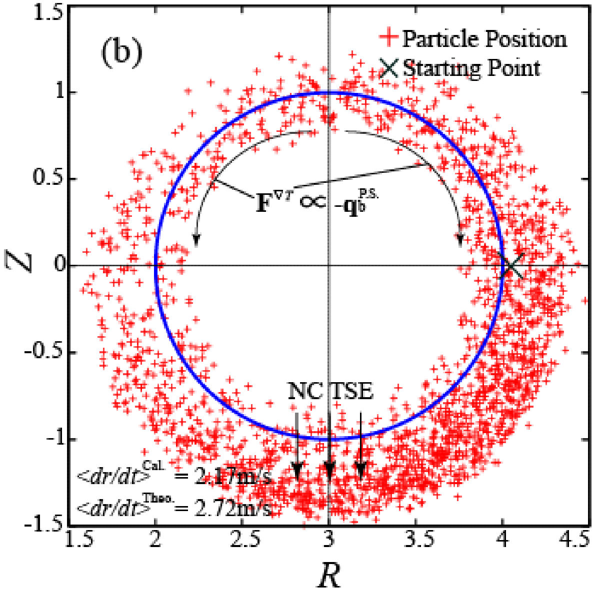

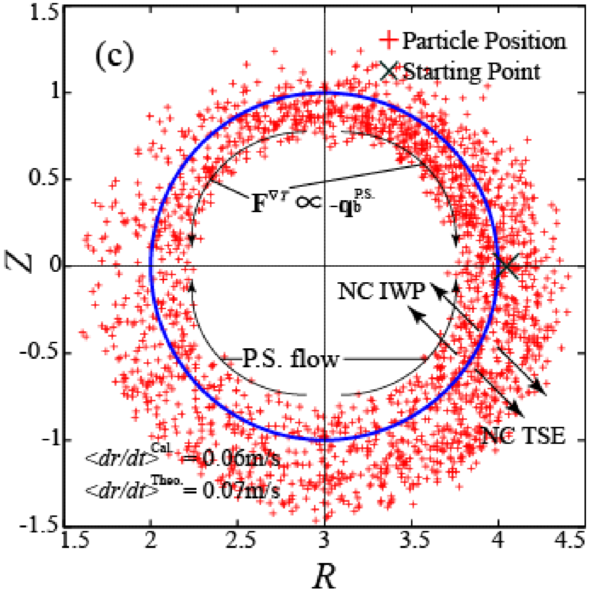

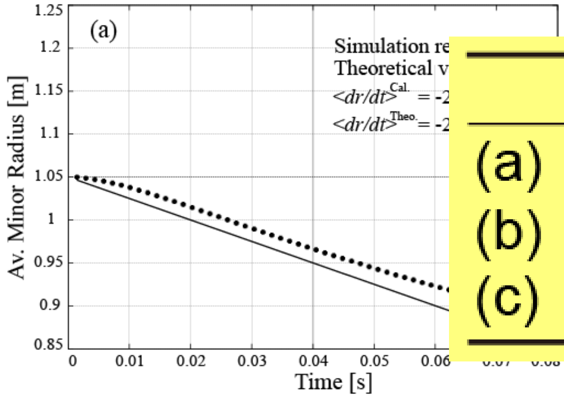

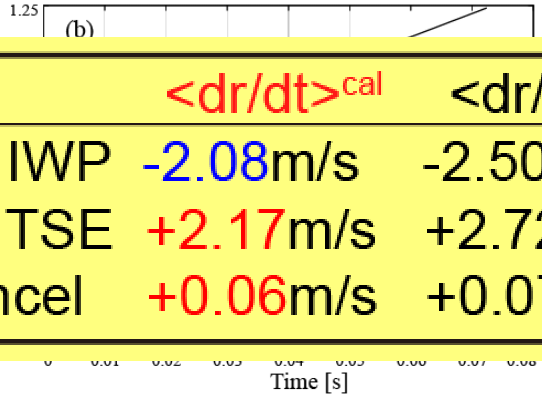

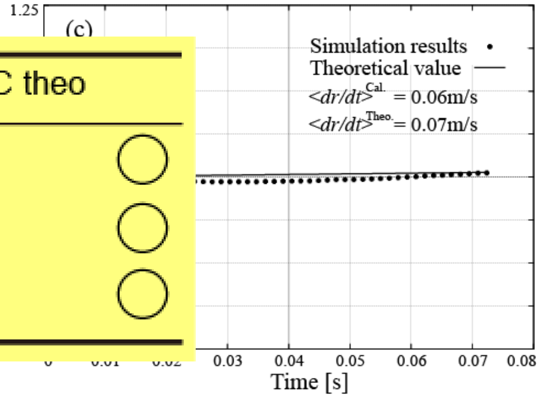

	$\langle dr/dt\rangle^{cal}$	$\langle dr/dt\rangle^{NC\ theo}$	
(a) NC IWP	-2.08m/s	-2.50m/s	○
(b) NC TSE	+2.17m/s	+2.72m/s	○
(c) Cancel	+0.06m/s	+0.07m/s	○

5. Conclusion and Future plan

- In a torus background plasma in Pfirsch-Schluter collisionality, our kinetic model can simulate the NC IWP and TSE.

  Important improvement in transport modeling!

- Implement in IMPGYRO code is underway.

- Aiming for more reliable analysis and suggestion to efficient way of impurity control in fusion devices!

6. References

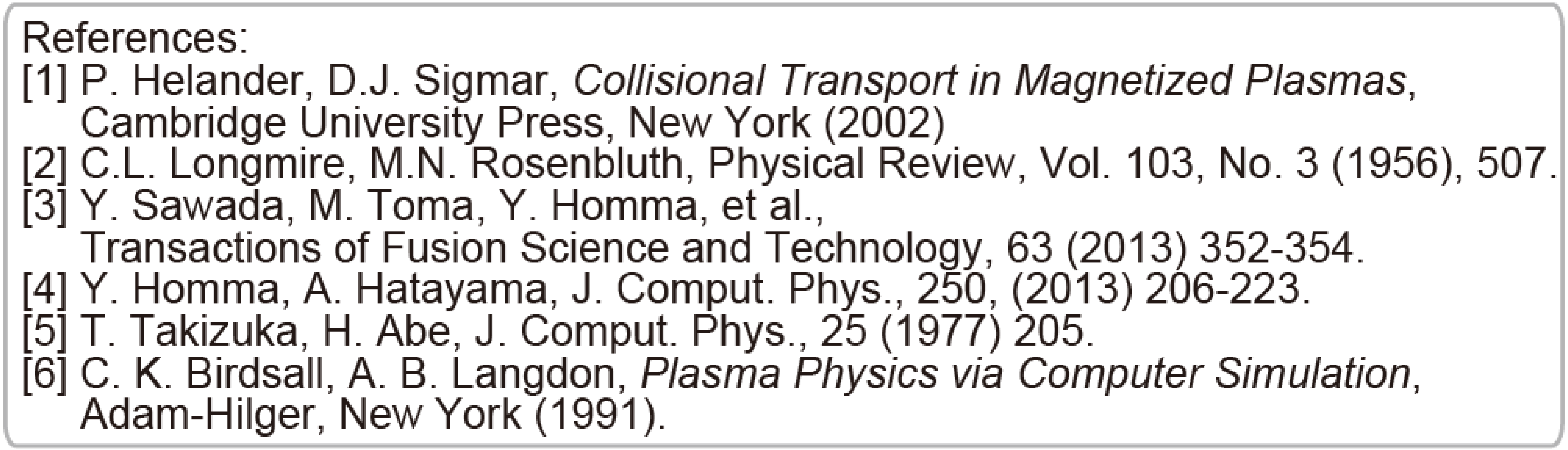

References:

[1] P. Helander, D.J. Sigmar, *Collisional Transport in Magnetized Plasmas*, Cambridge University Press, New York (2002)

[2] C.L. Longmire, M.N. Rosenbluth, Physical Review, Vol. 103, No. 3 (1956), 507.

[3] Y. Sawada, M. Toma, Y. Homma, et al., Transactions of Fusion Science and Technology, 63 (2013) 352-354.

[4] Y. Homma, A. Hatayama, J. Comput. Phys., 250, (2013) 206-223.

[5] T. Takizuka, H. Abe, J. Comput. Phys., 25 (1977) 205.

[6] C. K. Birdsall, A. B. Langdon, *Plasma Physics via Computer Simulation*, Adam-Hilger, New York (1991).

[7] Yuki Homma, Akiyoshi Hatayama, Contributions to Plasma Physics **54** (2014) No. 4-6, 394-398.

Thank you very much for listening!

Our current project: *Impurity transport simulation of the ITER-like plasma by the coupled SOLPS-IMPGYRO codes*
@ITER BA IFERC CSC "Helios" High Performance Computer
(Int. Fusion Energy Research Centre : Computer Simulation Centre),
Joint proposal: Keio Univ., Univ. Paris 13, IPP Garching, Greifswald Univ., JAEA.

Our recent publications:

"Numerical modeling of the thermal force for the kinetic test-ion transport simulation based on the Fokker-Planck collision operator"
Y. Homma, A. Hatayama, Contrib. Plasma Phys. **54** (2014) No. 4-6, 394-398.

"*Systematic Study of Tungsten Impurity Transport in Representative Regimes of Divertor Plasma*"
S. Yamoto, K. Hoshino, M. Toma, Y. Homma, A. Hatayama, X. Bonnin, D. Coster, R. Schneider, Contrib. Plasma Phys. **54** (2014) No. 4-6, 421-425.

"*Comparison of kinetic and fluid models for tungsten impurity transport using IMPGYRO and SOLPS"*
M. Toma, X. Bonnin, Y. Sawada, Y. Homma, A. Hatayama, K. Hoshino, D. Coster, R. Schneider, J. Nucl. Mater. **438** (2013) S620 – S624.

"*Numerical Modeling of Thermal Force in a Plasma for Test-Ion Transport Simulation Based upon Monte Carlo Binary Collision Model*" Y. Homma, A. Hatayama, J. Comput. Phys. **231** (2012) 3211-3227.

"*Numerical modeling of the thermal force in a plasma for test-ion transport simulation based on a Monte Carlo Binary Collision Model (II) -- Thermal forces due to temperature gradients parallel and perpendicular to the magnetic field --*" Y. Homma, A. Hatayama, J. Comput. Phys. **250** (2013) 206-223.